Available online at www.sciencedirect.com
ScienceDirect
Optical Materials 29 (2007) 556–561
OPTICAL Materials
www.elsevier.com/locate/optmat

Bismuth-doped zinc aluminosilicate glasses and glass-ceramics with ultra-broadband infrared luminescence

Mingying Peng [a,b,*], Danping Chen [a], Jianrong Qiu [a,c,*], Xiongwei Jiang [a], Congshan Zhu [a]

[a] Shanghai Institute of Optics and Fine Mechanics, Chinese Academy of Sciences, Photon Craft Project, 295#, Tacheng Road, Jiading, Shanghai 201800, China
[b] Graduate School of the Chinese Academy of Sciences, Beijing 100039, China
[c] Department of Materials Science and Engineering, Zhejiang University, Hangzhou 310027, China

Received 16 January 2005; accepted 5 August 2005
Available online 5 January 2006

Abstract

Broadband infrared luminescence covering the optical telecommunication wavelength region of O, E and S bands was observed from bismuth-doped zinc aluminosilicate glasses and glass-ceramics. The spectroscopic properties of the glasses and glass-ceramics depend on the thermal-treatment history. With the appearance of gahnite ($ZnAl_2O_4$) crystalline phase, the fluorescent peak moves to longer wavelength, but the fluorescent intensity decreases. The ~1300 nm fluorescence with a FWHM larger than 250 nm and a lifetime longer than 600 μs possesses these optical materials with potential applications in laser devices and broadband amplifiers. The broad infrared luminescence from the bismuth-doped zinc aluminosilicate glasses and glass-ceramics might be from BiO or bismuth clusters rather than from Bi^{5+} and Bi^{3+}.

PACS: 42.60.D; 42.70.C; 42.70.K; 42.79.S; 78.60

Keywords: Infrared luminescence; Glasses and glass-ceramics; Bismuth

1. Introduction

During past decades, transparent glass-ceramic as a new type of functional material has attracted much more and more attentions because of its wide application in the areas of flat panel displays, solar concentrators, optical amplifiers and up-conversion devices, etc. [1–5]. The studies on active ions, e.g., Ni^{2+} and Er^{3+}, activated glass-ceramics with high luminescent efficiency have been extensively performed and some promising results have been achieved [3–5].

In recent years, expanding the gain bandwidths of the fiber amplifiers and the laser sources to achieve more efficient wavelength division multiplexing transmission network with higher capacity and faster bit rate has become a key and attractive object for the future development of the optical communication. In order to further develop new amplifiers or lasers with much broader bandwidth, it is essential to explore new luminescent materials especially covering the 1200–1600 nm region. Recently, a novel broadband infrared luminescence in 1.2–1.6 μm was observed with a FWHM larger than 200 nm and a lifetime longer than 200 μs from bismuth-doped SiO_2 and GeO_2 glasses at room temperature [6,7]. The excellent optical properties for the new bismuth-activated materials make them as the good candidates for the super-broadband amplification gain media [6,7].

In this paper, we report the observation of broadband luminescence in 1.2–1.6 μm region from bismuth-doped zinc aluminosilicate glasses and glass-ceramics, study the

* Corresponding authors.
E-mail addresses: mypeng@mail.siom.ac.cn (M. Peng), jrq@photon.jst.go.jp (J. Qiu).

0925-3467/$ - see front matter © 2005 Elsevier B.V. All rights reserved.
doi:10.1016/j.optmat.2005.08.049

dependence of optical properties of the glasses and the glass-ceramics on the heat-treatment conditions and finally discuss the infrared fluorescence mechanism.

2. Experimental

Analytic reagents, MgO, ZnO, $SrCO_3$, $BaCO_3$, $NaNO_3$, SiO_2, $Al(OH)_3$, H_3BO_3, ZrO_2, TiO_2 and Bi_2O_3 were selected as raw materials. The selected glass compositions (in mol.%) were (1) $57.3SiO_2 \cdot 26.2AlO_{1.5} \cdot 10.6ZnO \cdot 0.9BaO \cdot 4.0TiO_2 \cdot 1.0Bi_2O_3$ (glass 1, hereafter), (2) $59.4SiO_2 \cdot 22.9AlO_{1.5} \cdot 6.8ZnO \cdot 3.8MgO \cdot 0.9BaO \cdot 3.9TiO_2 \cdot 1.5ZrO_2 \cdot 1.0Bi_2O_3$ (glass 2, hereafter) and (3) $30Na_2O \cdot 10Al_2O_3 \cdot 59SiO_2 \cdot 1.0Bi_2O_3$ (NASB glass, hereafter). The 150 g batches corresponding to glass 1 and glass 2, respectively, were weighted and thoroughly homogenized in an alumina mortar, and then melted for one and half hours at 1600 °C in alumina crucibles in air. The melts were cast onto a stainless steel plate and then annealed at 700 °C for 2 h. Each obtained glass sample was cut and polished into pieces with the size of $5 \times 5 \times 2\ mm^3$ for different heat-treatment processes in a small programmed electric furnace. The glass samples were heat treated in the following programs: 25 °C $\overset{240\ min}{\rightarrow}$ 700 °C $\overset{240\ min}{\rightarrow}$ 700 °C $\overset{100\ min}{\rightarrow}$ 850 °C $\overset{60\ min}{\rightarrow}$ 850 °C $\overset{120\ min}{\rightarrow}$ 850 °C, 900 °C or 950 °C $\overset{120\ min}{\rightarrow}$ 850 °C, 900 °C or 950 °C $\overset{540\ min}{\rightarrow}$ 25 °C. The characterized symbols for the heat-treated samples were employed to clearly illuminate the thermal-treatment histories of the different samples. For example, 1-950-2 h meant that glass 1 was heat treated at 950 °C for 2 h. Hundred gram batch for NASB glass sample was weighted, ground, preheated at 1200 °C for 2 h and then melt at 1550 °C for 20 min. The melt was quenched onto the steel plate and annealed at 500 °C for 1 h. The NASB glass sample was also cut and polished for the measurements. The polycrystalline powder sample of $Sr_{0.95}B_4O_7$:0.05Bi was prepared as follows: stoichiometric amounts of $SrCO_3$ and H_3BO_3 together with 3 mol% excess of H_3BO_3 to compensate for B_2O_3 evaporation were mixed, ground, preheated at 700 °C in alumina crucible in air for 5 h and then sintered at 850 °C for 5 h twice after reground.

The differential thermal analysis (DTA) curves were obtained with a CRY-Z Differential Thermal Analyzer at a heating rate of 10 °C min^{-1}. Phase assemblages were characterized by a Bruker D4 X-ray diffractometer at 40 kV/20 mA with CuKα_1 ($\lambda = 1.5405$ Å) as a radiation source and identified on the basis of JCPDS standard cards (05-0669 for $ZnAl_2O_4$, 34-0133 for $BaTi_2O_5$ and 15-801 for SrB_4O_7). The optical absorption spectra and the infrared luminescence spectra of the samples were measured using JASCO V-570 spectrophotometer and ZOLIX SBP300 spectrofluorometer with InGaAs detector at the excitation of the 808 nm laser diode (LD), respectively. The emission and the excitation spectra were recorded on a JASCO FP-6500 fluorescence UV–Vis spectrofluorometer. The fluorescence lifetime measurements were carried out by exciting the sample with a modulated 808 nm LD. The signals detected by an InGaAs photodetector in TRIAX550 spectrofluorometer were recorded using a storage digital oscilloscope (Tektronix TDS3052). All the measurements were taken at room temperature.

3. Results and discussion

3.1. Thermal stabilities of glass 1 and glass 2

DTA curves of glass 1 and glass 2 are illustrated in Fig. 1. The glass transition temperature (T_g), crystallization onset temperature (T_x) and maximum crystallization temperature (T_c) are observed and marked in Fig. 1. The parameter, $\Delta T = T_x - T_g$, can be used to roughly estimate the glass thermal stability. If ΔT is larger than 100 °C, the glass can be considered to have good thermal stability [8]. As shown in Fig. 1, the values of ΔT for glass 1 and glass 2 are 127 and 122 °C, respectively, indicating these glass samples are stable against devitrification. Interestingly, the T_c peak noticeably becomes broaden and flatten with additions of MgO and ZrO_2.

3.2. X-ray diffraction (XRD) patterns

Fig. 2a and b present the XRD patterns of glass 1 and glass 2 before and after heat-treatments. No apparent diffraction peaks can be observed for both the untreated glass 1 and glass 2, implying that they are vitreous. After heat-treatments, the diffraction peaks attributable to the main crystal phase of $ZnAl_2O_4$ are observed from all the heat-treated samples, together with the appearance of $BaTi_2O_5$ phase (see Fig. 2). Furthermore, as the heat-treatment temperature goes up from 850, 900 to 950 °C, the diffraction peaks of $ZnAl_2O_4$ become stronger and sharper, which shows the increase in the crystallite size. The average crystallite size was calculated by the Sherrer's equation. The strongest diffraction peak around $2\theta = 37°$ corresponding to the (3 1 1) plane was selected for the calculations. The size changes from about 8, 11 to 14 nm and from 6, 9 to 13 nm for glass 1 and glass 2 heat-treated at 850, 900 or 950 °C, respectively.

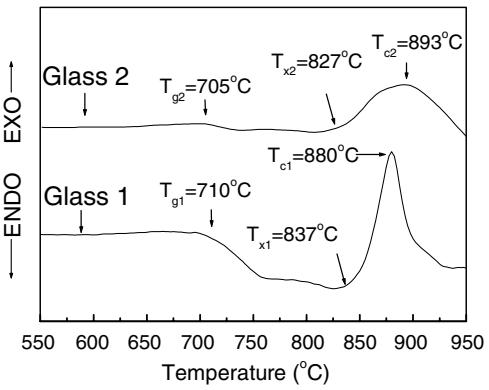

Fig. 1. DTA curves of glass 1 and glass 2.

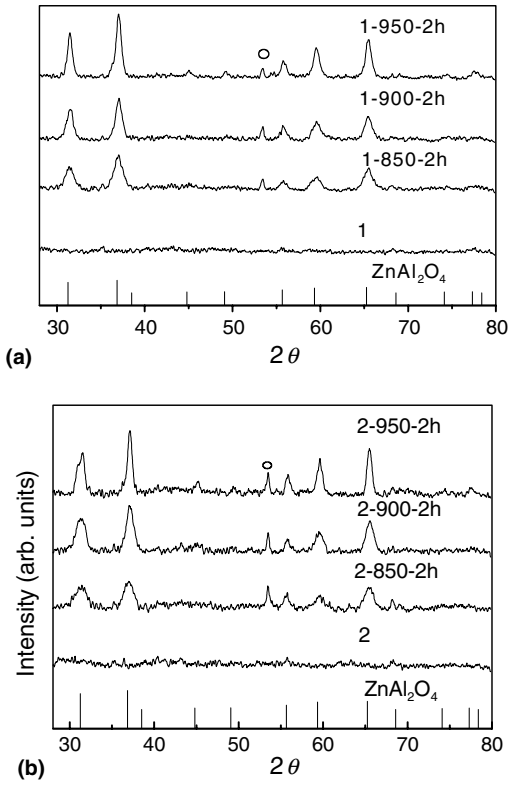

Fig. 2. X-ray diffraction patterns of (a) glass 1 and (b) glass 2 before and after heat-treatments. The bottom pattern is from Standard JCPDS card no. 05-0669 for $ZnAl_2O_4$. Open circle denotes the diffraction peak due to $BaTi_2O_5$.

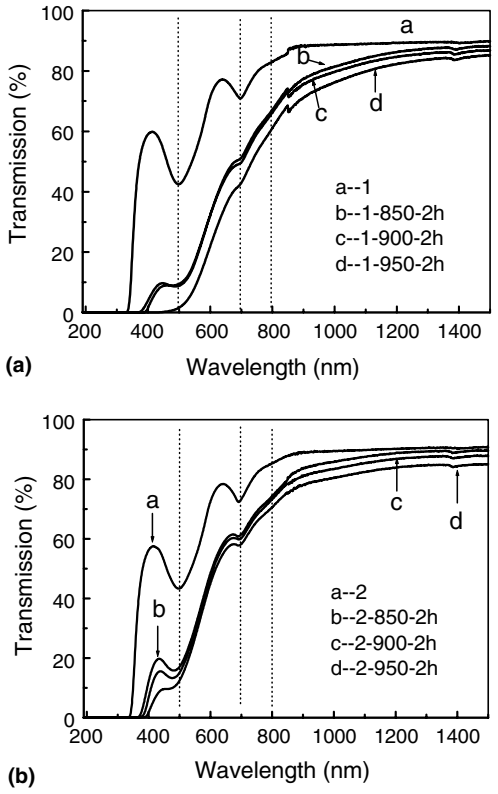

Fig. 3. Transmission spectra of (a) glass 1 and (b) glass 2 before and after heat-treatments.

3.3. Transmission spectra

Particle radii smaller than 15 nm and refractive index difference (Δn) smaller 0.1 between the glass and crystals are desirable to keep material with good transparency for the practical purposes [1]. As mentioned in Section 3.2, the crystalline particle radii are smaller than 15 nm. As reported in Ref. [1], Δn is less than 0.1. Thus, good transparency is preserved for the zinc aluminosilicate glasses and glass-ceramics (see Fig. 3). The maximum transmissions are close to 90% for the parent glass 1 and glass 2, but are a little lowered for the heat-treated specimens. As the heat-treatment temperature increases, the body color of sample turns from light reddish brown to reddish brown and transmission decreases in turn. Three absorption peaks at around 500, 700 and 800 nm should be assigned to the absorptions of bismuth ions [6,7].

3.4. Infrared fluorescence spectra

Fig. 4 shows the infrared fluorescence spectra of glass 1 and glass 2 before and after heat-treatments in the case of 808 nm excitation. There is a broadband peaked at around 1260 nm with FWHM of 286 nm for glass 1. With the appearance of $ZnAl_2O_4$ phase, the peak position suddenly moves to the longer wavelength of about 1285 nm with

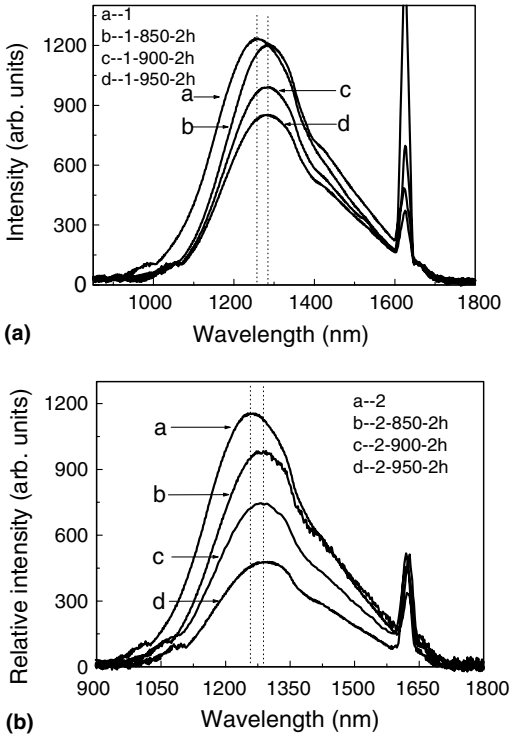

Fig. 4. Fluorescence spectra of (a) glass 1 and (b) glass 2 before and after heat-treatments pumped by 808 nm LD.

slight decrease in intensity. However, as the $ZnAl_2O_4$ nanoparticle further grows up, the 1285 nm peak remains unshifted and the intensity decreases continuously. For glass 2 and its heat-treated samples, the similar case appears as shown in Fig. 4b. The fluorescent peak lies at 1260 and 1290 nm for glass 2 and its heat-treated samples, respectively.

In the crystallizing course of the glasses, the active ions, e.g., Ni^{2+}, Cr^{3+} or Er^{3+}/Yb^{3+}, will enter the crystalline phase and therefore the luminescence intensity could be strongly enhanced for the glass-ceramics [3–5,9]. But based on our experiment results mentioned above, we propose that the bismuth ions still stay in the residual glass phase of the formed glass-ceramics. The larger radius difference between bismuth ions ($R_{Bi^{3+}} = 1.03$ Å) and the hosted cations ($R_{Zn^{2+}} = 0.74$ Å and $R_{Al^{3+}} = 0.39$ Å) might be the driving force to prevent bismuth ions from entering the gahnite phase.

All the previous investigations demonstrated that co-doping of aluminum into bismuth-doped glasses is indispensable for the broadband infrared luminescence [6,7]. Furthermore, in our former studies on GeO_2:Al,Bi glasses, we found that increasing the aluminum content will lead to the increase of the infrared fluorescence intensity. Though the real role of the aluminum ions in the generation of infrared luminescence is unknown up to now, it can be considered that such ions can homogenously disperse the bismuth ions throughout the glass host to some extent as they do in Al^{3+} and Nd^{3+} co-doped silica glass [10]. In silica glass, Al^{3+} ions surround Nd^{3+} ions with the bonding association of Al–O–Nd and enlarge the spacing between Nd^{3+} ions. And therefore the interaction between Nd^{3+} ions is weakened and the luminescence efficiency of Nd^{3+} ions is improved [10]. Compared with the untreated glass 1 and glass 2, the Al_2O_3 concentration as dispersant agent is relatively lower in the residual glass phase of heat-treated specimens, since a part of Al_2O_3 is consumed to form the $ZnAl_2O_4$ nanoparticles in the glass ceramics. So the interaction between bismuth ions becomes stronger in the glass-ceramics, which can be verified by the reduction of the fluorescence lifetime from 746 to 666, 631 and 616 μs for 1, 1-850-2 h, 1-900-2 h and 1-950-2 h, respectively, and the fluorescence intensities are therefore weakened as shown in Fig. 4.

3.5. Mechanism of infrared luminescence

Nowadays, it is still unknown where the broad infrared emission comes from in bismuth-doped glasses [6,7]. Obviously, the lifetime and the positions of both absorption and emission peaks of bismuth-doped SiO_2, GeO_2 and zinc aluminosilicate glasses quite differ from the Bi^{3+} or Bi^{2+} doped luminescent materials previously reported in literature [11–16]. For example, the lifetime in Bi^{3+}-doped sodium borate or phosphate glasses was less than 4 μs [15]. Fujimoto et al. ascribed the absorption and the emission spectra of SiO_2:Al, Bi to the Bi^{5+} transitions between the ground state of $^1S_0$ and the excited states of $^3D_{3,2,1}$ and $^1D_2$ [6]. However, at higher temperature, Bi_2O_3 will readily dissociate into the suboxide BiO or even into bismuth metal [17]. We suspect that the infrared luminescence with the lifetime longer than 600 μs might originate from the lower-valence bismuth but not from Bi^{5+} ion. In order to identify where the infrared luminescence came from, we prepared the transparent and colorless NASB glass and the light-pink polycrystalline sample of $Sr_{0.95}B_4O_7$:0.05Bi.

As well known, high-valent Bi^{5+} ion often exists in the compounds, e.g., $NaBiO_3$ or $KBiO_3$, containing alkali oxides with higher basicity [18,19]. The optical basicity calculated from the empirical formula proposed by Duffy [20,21] is 0.612 for the NASB glass, 0.515 for glass 1 and 0.516 for glass 2. According to the optical basicity theory [21], the upper oxidation state of dopant is usually favorable in glass with higher basicity. Thus, the higher valent Bi^{5+} ions should be more preferred in NASB glass than in glass 1 and glass 2. If the infrared luminescence comes from Bi^{5+} ions, the infrared emission should also be observed from NASB glass as well as from glass 1 and glass 2. However, no broad infrared emission but only the typical absorption and emission due to Bi^{3+} ions can be detected in the NASB glass with higher Na_2O content at room temperature as indicated in Fig. 5. So the infrared luminescence is not from Bi^{5+} and Bi^{3+} ions.

The compound of SrB_4O_7 possesses the strong reducing ability and the trivalent RE^{3+} ions (RE = Eu, Sm, Yb, Tm, Nd) built into this matrix can be easily reduced to RE^{2+} even though SrB_4O_7:RE is prepared in an oxidizing atmosphere of air (The trivalent Sm, Tm or Nd ions are usually difficult to be reduced to their divalent form in most of other host compounds even prepared in $N_2 + H_2$.) [16,22–24]. So it is possible that the Bi^{3+} ions doped into SrB_4O_7 are partially reduced to the lower-valence forms such as divalent ions (Standard electrode potential $\varphi^{\vartheta}(Sm^{3+}/Sm^{2+}) = -1.15$ V, $\varphi^{\vartheta}(Eu^{3+}/Eu^{2+}) = -0.429$ V, $\varphi^{\vartheta}(Bi^{3+}/Bi^{+}) = 0.20$ V, $\varphi^{\vartheta}(Bi^{3+}/Bi) = 0.308$ V). Blasse et al. reported the co-existence of Bi^{3+} and Bi^{2+} in SrB_4O_7, but they did not study the luminescence in the near infrared

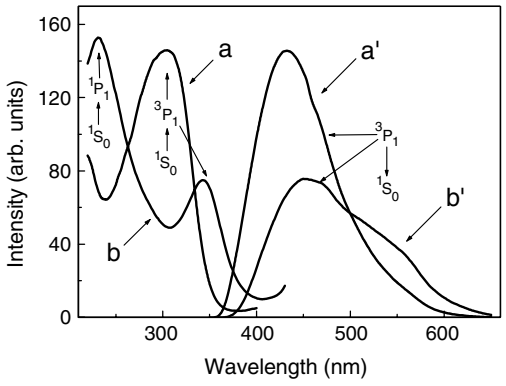

Fig. 5. Excitation and emission spectra of NASB glass (*a*: $\lambda_{em} = 433$ nm; *a*′: $\lambda_{ex} = 304$ nm) and glass 1 (similar to glass 2) (*b*: $\lambda_{em} = 452$ nm; *b*′: $\lambda_{ex} = 342$ nm). Assignments are based on Refs. [11–15].

region [16]. At the excitation of 808 nm-laser, a weak broadband emission in the region of 1100–1500 nm was observed from $Sr_{0.95}B_4O_7$:0.05Bi, implying that the infrared luminescence might initiate from lower-valent bismuth (see Fig. 6).

At high temperature, Bi_2O_3 can be partially converted into atomic bismuth metal [17]. If the resulting bismuth atoms have a chance to become aggregated, bismuth clusters like Bi_2 can be formed. Fink et al. found the emission in the spectral region of 7620 cm^{-1} (1312 nm) ~7800 cm^{-1} (1282 nm) from Bi_2 in gas phase, but they did not present the lifetime data [25]. Recently, Fink and Shestakov et al. discovered the $X_2\ ^2\Pi_{3/2} \rightarrow X_1\ ^2\Pi_{1/2}$ emissions in 1.0–1.6 μm with radiative lifetime of 480 ± 100 μs from BiO in gas phase [25,26]. In view of the similarity in emission-peak positions and lifetime between BiO in gas phase, glass 1 and glass 2, we propose that the infrared luminescence might be from BiO dissolved in glass 1 and glass 2. The more identified conclusion could not be made at this moment, because we cannot rule out the other possibility that the infrared luminescence origins from the bismuth cluster, e.g., Bi_2. Given that the infrared luminescence is really from BiO, the observed absorptions at ~500, 700 and 800 nm can be assigned to $X_1 \rightarrow$ (H, I), $X_1 \rightarrow A_2$ and $X_1 \rightarrow A_1$ respectively, and the emission peak at 1260 nm can be to $X_2 \rightarrow X_1$ [26].

In untreated glass 1 and glass 2, Bi^{3+} emissions are observed except the 1260 nm fluorescence (see Fig. 5); while in the heat-treated samples, no emissions from Bi^{3+} but only 1260 nm emission can be found, which proves that the 1260 nm fluorescence is not from Bi^{3+}. Maybe, the trivalent bismuth ions are reduced to lower valence state in the heat-treated samples. As compared with untreated glass 1 and glass 2, the infrared-fluorescence intensities of the heat-treated samples are evidently lowered, which might be interpreted by the following three reasons: (1) the decrement of dispersing agents of Al_2O_3 in the glass phase of the heat-treated samples leads to the interaction enhancement between the activators as discussed in Section 3.4; (2) the bismuth-concentration increasing in the glass phase of the heat-treated samples results in concentration-quenching, because bismuth cannot be built into the $ZnAl_2O_4$ phase; (3) the pump energy loss due to the pumping light scattering increases as nanocrystals grow up.

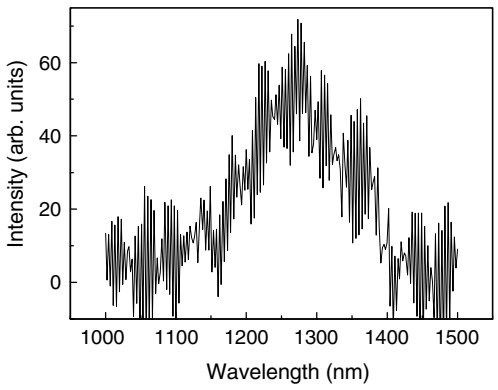

Fig. 6. Fluorescence spectrum of $Sr_{0.95}B_4O_7$:0.05Bi prepared in air when pumped by 808 nm LD.

4. Conclusions

Broadband infrared luminescence covering O (1260–1360 nm), E (1360–1460 nm) and S (1460–1530 nm) bands in the optical telecommunication region was observed from bismuth-doped zinc aluminosilicate glasses and glass-ceramics. The fluorescent intensity, lifetime and peak position depend on the thermal-treatment history. With the appearance of gahnite ($ZnAl_2O_4$) crystalline phase, fluorescent peak moves to longer wavelength. The broad ~1300 nm fluorescence with FWHM larger than 250 nm and lifetime longer than 600 μs possesses these optical materials with potential applications in laser devices and broadband amplifiers. The broad infrared luminescence from bismuth-doped zinc aluminosilicate glasses and glass-ceramics might be from BiO or bismuth clusters rather than from Bi^{5+} and Bi^{3+}.

Acknowledgements

Mingying Peng would like to thank Prof. E.H. Fink for helpful discussions about mechanism analysis during the development of this article. This work is financially supported by the National Natural Science Foundation of China (Grant No. 50125258, 20504026 and 60377040), Shanghai Committee of Science and Technology (Grant No. 04XD14018), Shanghai Nanotechnology Promotion Center (Grant No. 0352 nm042) and the State Key Lab for Advanced Photonic Materials and Devices, Fudan University.

References

[1] G.H. Beall, L.R. Pinchney, J. Am. Ceram. Soc. 82 (1) (1999) 5.
[2] L.R. Pinchney, J. Non-Cryst. Solids 255 (1999) 171.
[3] K. Tanaka, T. Mukai, T. Ishihara, K. Hirao, N. Soga, S. Sogo, M. Ashida, R. Kato, J. Am. Ceram. Soc. 76 (11) (1993) 2839.
[4] B.N. Samson, L.R. Pinckney, J. Wang, G.H. Beall, N.F. Borrelli, Opt. Lett. 27 (15) (2002) 1309.
[5] Y. Wang, J. Ohwaki, Appl. Phys. Lett. 63 (24) (1993) 3268.
[6] Y. Fujimoto, M. Nakatsuka, Jpn. J. Appl. Phys. 40 (2001) L279.
[7] M. Peng, J. Qiu, D. Chen, X. Meng, L. Yang, X. Jiang, C. Zhu, Opt. Lett. 29 (17) (2004) 1998.
[8] L. Neindre, S. Jiang, B. Hwang, T. Luo, J. Watson, N. Peyghambarian, J. Non-Cryst. Solids 255 (1999) 97.
[9] G. Boulon, Mater. Chem. Phys. 16 (1987) 301.
[10] I. Thomas, S. Payne, G. Wilke, J. Non-Cryst. Solids 151 (1992) 183.
[11] G. Boulon, B. Moine, J. Bourcet, R. Reisfeld, Y. Kalisky, J. Lumin. 18 (19) (1979) 924.
[12] R. Reisfeld, L. Boehm, J. Non-Cryst. Solids 16 (1974) 83.
[13] Z. Pei, Q. Su, J. Zhang, Solid State Commun. 86 (6) (1993) 377.
[14] D. Van de Voort, G. Blasse, J. Solid State Chem. 99 (1992) 404.
[15] S. Parke, R.S. Webb, J. Phys. Chem. Solids 34 (1973) 85.
[16] G. Blasse, A. Meijerink, M. Nomes, J. Zuidema, J. Phys. Chem. Solids 55 (2) (1994) 171.

[17] M.B. Volf, in: Chemical Approach to GlassGlass Science and Technology, vol. 7, Elsevier Science Publishing Company, 1984, p. 465.
[18] R. Retoux, F. Studer, C. Michel, B. Raveau, A. Fontaine, E. Dartyge, Phys. Rev. B 41 (1) (1990) 193.
[19] S. Salem-Sugui Jr., E.E. Alp, S.M. Mini, M. Ramanathan, J.C. Campuzano, G. Jennings, M. Faiz, Phys. Rev. B 43 (7) (1991) 5511.
[20] J.A. Duffy, M.D. Ingram, J. Non-Cryst. Solids 21 (1976) 373.
[21] J.A. Duffy, J. Non-Cryst. Solids 196 (1996) 45.
[22] Z. Pei, Q. Su, J. Zhang, J. Alloy Compd. 198 (1993) 51.
[23] J. Peterson, W. Xu, S. Dai, Chem. Mater. 7 (9) (1995) 1686.
[24] W. Xu, J. Peterson, J. Alloy Compd. 249 (1997) 213.
[25] E.H. Fink, K.D. Setzer, D. Ramsay, M. Vervloet, Chem. Phys. Lett. 179 (1991) 103.
[26] O. Shestakov, R. Breidohr, H. Demes, K.D. Setzer, E.H. Fink, J. Mol. Spectrosc. 190 (1998) 28.